Electronic Supplementary Material (ESI) for Green Chemistry.

One-pot, template-free synthesis of robust superhydrophobic polymer monolith with adjustable hierarchical porous structure

Yong Li [a,b], Zhaozhu Zhang [a*], Bo Ge [a,b], Xuehu Men [c*], and Qunji Xue [a]

[a] State Key Laboratory of Solid Lubrication, Lanzhou Institute of Chemical Physics, Chinese Academy of Sciences, Tianshui Road 18th, Lanzhou 730000, PR China.

[b] University of Chinese Academy of Sciences, Beijing 100039, PR China.

[c] School of Physical Science and Technology, Lanzhou University, Lanzhou, 730000, P. R. China

[*] Corresponding author. Tel.: +86 931 4968098
E-mail address: zzzhang@licp.cas.cn (Z. Z); menxh@lzu.edu.cn (X. H. Men)

Movie S1. Movie illustrates that the superhydrophobic polymer monolith suffers from water impact by a strong water flow for more than 8 min.

Movie S2. The polymer monolith can be used for painting superhydrophobic surface on both planar and tender substrates like a chalk. The painted sandpaper, copper mesh, latex glove and A4 paper show excellent superhydrophobicity.

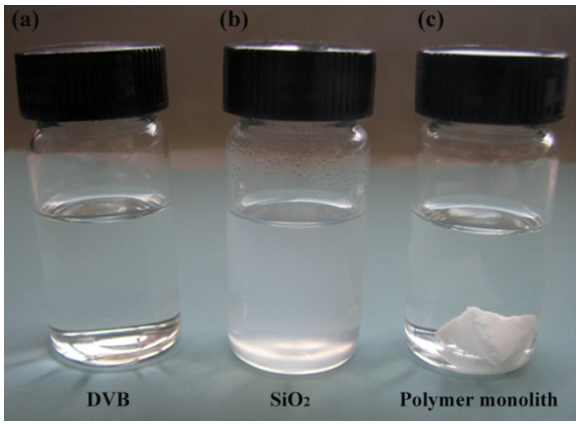

Figure S1 Photos of DVB, SiO_2 and polymer monolith dissolved in ethyl acetate.

As shown in Figure S1, DVB monomers were completely dissolved in ethyl acetate and good dispersion was found for SiO_2, whereas, no dissolution can be found for polymer monolith in ethyl acetate.

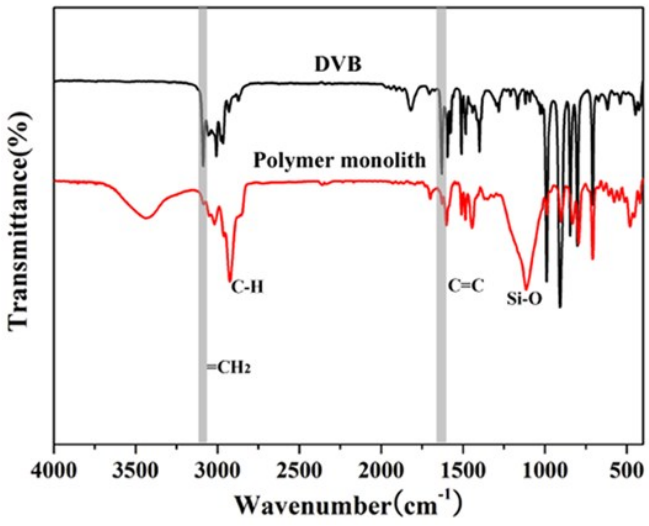

Figure S2 FT-IR spectra of the PDVB-SiO_2-110 samples

Table S1 BET surface area and pore volume of all samples prepared under different solvothermal temperature

Temperature (°C)	BET specific surface area (m^2/g)	Pore volume (cm^3/g)
60	602.5	1.15
80	675.5	1.35
100	762.8	1.52
110	820.5	1.59
120	792.0	1.54
140	741.4	1.40

The related structure and performances of polymer monoliths containing different amount of SiO_2 nanoparticles

In our study, SiO_2 nanoparticles were used mainly as a mechanically reinforced material and could increase the BET surface area and pore volume of polymer monolith. The related structure and performances were characterized after adjust the amount of SiO_2. Firstly, the polymer monoliths containing different content of SiO_2 particles were obtained at the solvothermal temperature of 110 °C to investigate mechanical enhancements. All the obtained polymer monoliths take on white color and cylinder morphology (hence denoted as PDVB-SiO_2-x, x is the mass of SiO_2, x= 0, 0.1, 0.2, 0.3, 0.4). However, PDVB-SiO_2-0.4 sample is fragile and crack can be observed obviously, which indicates low mechanical strength (Fig. S3b). The axial compressive stress of other samples was provided by an electronical universal material testing machine DY35. As shown in Table S2, the compressive stress increases with respect to the pure PDVB (2.6×10^5 Pa) alone by increasing the amount of SiO_2. The compressive stress increases to 2.9×10^5 Pa for PDVB-SiO_2-0.1 and up to

3.3×10^5 Pa for PDVB-SiO_2-0.2, which is contributed by the mechanical reinforcing effect of SiO_2 nanoparticles. While further increasing the content of SiO_2 particles would decrease its mechanical strength. The compressive stress of PDVB-SiO_2-0.3 decreases to 2.0×10^5 Pa even lower than pure PDVB monolith. Therefore, definite SiO_2 nanoparticles can reinforce mechanical properties of polymer monolith. The reinforce properties result from high dispersion and the mechanical reinforcing effect of fumed SiO_2 nanoparticles. The SiO_2 particles can uniformly embedded in PDVB during the polymerization, which result in uniform stress distribution and minimizes the presence of stress concentration center.[1,2] Whereas, excessive SiO_2 nanoparticles lead to aggregate and increase stress concentration center which caused a fragile monolith.

Secondly, we focused on their influence on the porosity of polymer monoliths Fig. S4 shows N_2 isotherms and pore size distribution of PDVB-SiO_2-x (x is the mass of SiO_2, x= 0, 0.1, 0.2, 0.3). All these samples behave H4 hysteresis loop and a slow increase in the adsorption amount occurs during the relative pressure range of 0.4-0.8, indicating the presence of mesopores. Significantly, the nitrogen adsorption capacity still increases at high relative pressure (P/P_0 >0.8) indicating the presence of large pores. Pore size distribution of all samples estimated from desorption branches of the isotherms[3] reveals that the hierarchical porosity mainly ranges from 10-100 nm, indicating broad size distributions (Fig. S4b). Their BET surface area and pore volume were shown in Table S2, all the samples show large BET surface areas (728.7-820.5 m^2/g) and high pore volume (1.39-1.59 m^3/g). PDVB-SiO_2-0.2 exhibits

highest BET surface area (820.5 m^2/g) and pore volume (1.59 cm^3/g). This should be attributed to the definite SiO_2 nanoparticles can reduce the shrink during the removal of ethyl acetate and benefit the formation of pores. Hence, SiO_2 nanoparticles mainly as a mechanically reinforced material as well as benefit improving BET surface area and pore volume. PDVB-SiO_2-0.2 is the optimal conditions for fabricating hierarchically porous polymer monoliths with highest BET surface area and pore volume.

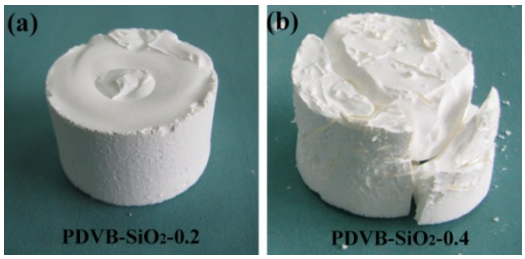

Figure. S3 Images of polymer monolith (a) PDVB-SiO_2-0.2 and (b) PDVB-SiO_2-0.4

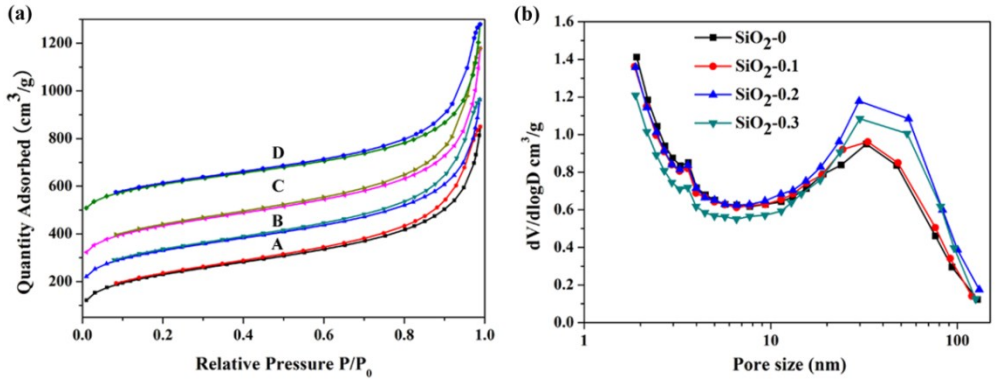

Figure. S4 (a) N_2 isotherms and (b) pore size distribution of (A) PDVB-SiO_2-0, (B) PDVB-SiO_2-0.1, (C) PDVB-SiO_2-0.2, (D) PDVB-SiO_2-0.3, samples. Isotherms of (B)-(D) have been offset by 100 cm^3/g, 200 cm^3/g and 400 cm^3/g, respectively, along the vertical axis for clarity.

Table S2 Compressive stress, BET surface area and pore volume of all samples containing different content of SiO_2 nanoparticles

Samples	Compressive stress (Pa)	S_{BET} (m^2/g)	Pore volume (cm^3/g)
PDVB-SiO_2-0	2.6×10^5	801.2	1.39
PDVB-SiO_2-0.1	2.9×10^5	805.2	1.41
PDVB-SiO_2-0.2	3.3×10^5	820.5	1.59
PDVB-SiO_2-0.3	2.0×10^5	728.7	1.42

Table S3 The comparison between present work and previous reported polymer or carbon aerogels and porous polymer

Materials	Method	S_{BET} (m^2/g)	WCA	Highlight and comments
Elastic carbon foam[4]	Pyrolysis of melamine sponge	268		High porosity, excellent elasticity harsh conditions
CNT sponge[5]	CVD	300- 400	156°	High-porosity, mechanical stability, special equipment , high cost
Carbon nanofiber aerogel[6]	Template hydrothermal method, freeze-drying and pyrolysis	547	136°	High sorption capacity, mechanical stability, multistep procedures, harsh conditions
TCF aerogel[7]	Pyrolysis of cotton			Natural source, strong sorption capability, high temperature and poor mechanical performance
Spongy graphene[8]	Freeze-drying and high temperature reduction		153°	Excellent absorption capacity, multistep procedures, high cost, low mechanical stability

Graphene/carbon nanotube hybrid foam[9]	CVD and templating method	Macroporous	152.3°	Macroporous structure, high oil capacity, special equipment, multistep procedures, chemical etching
Magnetic Cellulose Sponge[10]	Templating method, freeze-drying, extra modification		156°	W/O emulsions separation, multistep procedures, time-consuming and special equipment
Porous Polymer Coatings[11]	Photoinitiated copolymerization in the presence of porogens		172°	Applied to various surfaces, time-saving, low adhesive with substrates and easily damaged
Macroporous PDMS/MWNT Nanocomposite[2]	Templating method	Macroporous	153.4°	Magnetic properties, improved mechanical properties, relative low oil capacity, hard template
Silanized melamine sponges[12]	Solution-immersion method	Macroporous	151°	Cost-effective, recyclable oil capacity
Melamine sponge[13]	two-step immersion coating	Macroporous	163°	Flame-retardant and oil removal, expensive and harmful fluorinated material
PU@Fe3O4@SiO_2 @FP Sponges[14]	CVD and dip-coating	Macroporous	157°	Magnetic, oil removal, multistep procedures, low oil capacity
PDMS Sponges[15]	Templating method		151.5°	Selective Oil Absorption, high compressibility and stretchability, hard template needed
Magnetic foams[16]	Pyrolyzing polyelectrolyte grafted polyurethane sponge		152°	Magnetic, high oil capacity, ultralow-density, time-consuming, high temperature
Porous polymers[17]	Polymerization of the vinyl monomers using hard template	82.4		Hierarchical porous structures low oil capacity, hard template needed
Porous PDVB-SiO_2 monolith (our work)	Solvothermal method in the absence of template, surfactant or stabilizer	820.5	161.3°	Tunable hierarchical porosity, durable superhydrophobic property, environment benign

Abrasion test

To check the robustness of the polymer monolith against mechanical forces, an abrasion test have been performed. Figure S5 illustrates the method of the abrasion test: 800 mesh sandpaper served as an abrasion surface. The coated fabric was subjected to a1.0 kg weight and was kept in close contact with the sandpaper. Then the polymer monolith sample was dragged in one direction with a speed and abrasion length of 2 cm/s^{-1} and 10 cm, respectively.

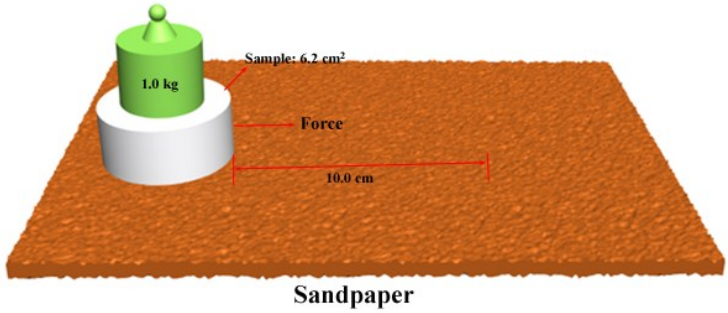

Figure S5 Schematic illustration of the methodologyof the abrasion test.

Reference

1. X. Z. Ye, H. Wang, K. Zheng, Z. F. Wu, H.F. Zhou, K. H. Tian, Z. Su, X. Y. Tian, Composites Science and Technology, 2016, **124**, 1-9.
2. A. Turco, C. Malitesta, G. Barillaro, A. Greco, A. Maffezzoli, E. Mazzotta, J. Mater. Chem. A, 2015, **3**, 17685-17696.
3. M. Kruk, M. Jaroniec, Chem. Mater, 2003, **15**, 2942-2949.
4. S. L. Chen, G. H. He, H. Hu, S. Q. Jin, Y. Zhou, Y. Y. He, S. J. He, F. Zhao, H. Q. Hou, Energy Environ. Sci., 2013, **6**, 2435-2439.
5. X. C. Gui, J. Q. Wei, K. L. Wang, A. Y. Cao, H. W. Zhu, Y. Jia, Q. K. Shu, D. H. Wu, Adv. Mater., 2010, **22**, 617-621.
6. Z. Y. Wu, C. Li, H. W. Liang, Y. N. Zhang, X. Wang, J. F. Chen, S. H. Yu, Sci. Rep., 2014, **4.**
7. H. Bi, Z. Yin, X. Cao, X. Xie, C. Tan , X. Huang , B. Chen, F. Chen , Q. Yang, X. Bu, X. Lu, L. Sun, H. Zhang, Adv. Mater., 2013, **25**, 5916-5921.
8. H. C. Bi, X. Xie, K. B. Yin, Y. L. Zhou, S. Wan, R. S. Ruoff, L. T. Sun, J. Mater. Chem. A, 2014, **2**, 1652-1656
9. X. C. Dong, J. Chen, Y. W. Ma, J. Wang, M. B. Chan-Park, X. M. Liu, L. H. Wang, W. Huang, P. Chen, Chem. Commun., 2012, **48**, 10660-10662.
10. H. L. Peng, H. Wang, J. N. Wu, G. H. Meng, Y. X. Wang, Y. L. Shi, Z. Y. Liu, X. Guo, Ind. Eng. Chem. Res. 2016, **55**, 832-838.
11. P. A. Levkin, F. Svec, J. M. J. Frechet, Adv. Funct. Mater., 2009, **19**, 1993-1998.
12. V. H. Pham and J. H. Dickerson, ACS Appl. Mater. Interfaces, 2014, **6**, 14181-14188.

13. C. P. Ruan, K. L. Ai, X. B. Li, L. H. Lu, Angew. Chem. Int. Ed., 2014, **53**, 5556 - 5560.

14. L. Wu, L. X. Li, B. C. Li, J. P. Zhang, A. Q. Wang, ACS Appl. Mater. Interfaces, 2015, **7**, 4936-4946.

15. X. Zhao, L. X. Li, B. C. Li, J. P. Zhang, A. Q. Wang, J. Mater. Chem. A, 2014, 2, 18281-18287.

16. N. Chen, Q. M. Pan, ACS Nano, 2013, **7**, 6875-6883.

17. K. Sato, Y. Oaki, H. Imai, Chem. Commun., 2015, **51**, 7919-7922.